# Blowup solutions of the Korteweg-de Vries equation

Vivi Rottschäfer and Corine Meerman
Mathematical Institute
Leiden University
P.O. Box 9512
2300 RA Leiden, The Netherlands
and
Paul A. Zegeling
Mathematical Institute
Utrecht University
P.O. Box 80010
3508 TA Utrecht, The Netherlands

**Abstract**

In this article we construct, both asymptotically and numerically, blowup solutions to the Generalised Korteweg-de Vries equation (GKdV). It has been known that for a certain choice of nonlinearity, solitary waves of the GKdV can become unstable and become infinite in finite time, in other words blow up. We find that in our numerical simulations, the solitary waves travel to the right with an increasing speed, and simultaneously, seem to form a similary structure after which they blow up. Based on these observations, we rescale the GKdV to the equation that will be analysed by using asymptotic methods, and thereby resolve the complete structure of these blowup solutions. In both the numerics and the asymptotics, we find that the solution has sech-like behaviour near the peak. Moreover, it becomes asymmetric with exponential decaying behaviour to the right and algebraic decay to the left of the peak.

keywords: Generalised Korteweg-de Vries equation; Blowup solutions.

## 1 Introduction

In this article, we analyse the Generalized Korteweg-de Vries (GKdV) equation of the following form

$$\frac{\partial \phi}{\partial t} + \frac{\partial}{\partial x}\left(\frac{\partial^2 \phi}{\partial x^2} + \phi^p\right) = 0, \tag{1.1}$$

where $\phi, x \in \mathbf{R}$, $t > 0$, $p$ is a positive parameter and with initial condition

$$\phi(x, 0) = \phi_0(x).$$

This equation arises in modelling the propagation of small-amplitude waves in a variety of nonlinear dispersive media, where $\phi$ represents the wave amplitude, see [4, 3]. Moreover, the equation is shown to describe the behaviour of longitudinal waves propagating in a one-dimensional lattice of equal masses coupled by nonlinear springs; the Fermi, Pasta, Ulam (FPU)-lattice, see [22] and references therein. The special case $p = 2$ gives the classical Korteweg-de Vries equation (KdV) which was posed by Korteweg and de Vries [9] to describe water waves on shallow water. The case $p = 3$, which is known as the Modified Korteweg-de Vries equation, can be transformed into the original Korteweg-de Vries equation by the Miura transformation, [1].

Together with the nonlinear Schrödinger equation, this equation can be considered as a universal model for Hamiltonian systems in infinite dimensions. Since equation (1.1) is Hamiltonian, there is conservation of energy, where the energy is given by

$$\begin{aligned} E(\phi(t)) &= \frac{1}{2}\int_{\mathbf{R}} \left[\phi_x(x,t)^2 - \frac{1}{p+1}\phi(x,t)^{p+1}\right] dx \qquad (1.2)\\ &= \frac{1}{2}\int_{\mathbf{R}} \left[\phi_x(x,0)^2 - \frac{1}{p+1}\phi(x,0)^{p+1}\right] dx. \end{aligned}$$

Moreover, the mass, given by

$$M(\phi(t)) = \int_{\mathbf{R}} \phi(x,t)^2 dx, \qquad (1.3)$$

is also conserved, so

$$M(\phi(t)) = \int_{\mathbf{R}} \phi(x,0)^2 dx.$$

In this article, we study solutions of equation (1.1) that become infinite in finite time, hence they blow up. Depending on the choice of $p$, the power of the nonlinearity, blowup solutions indeed exist. The cases $p = 2$ and $p = 3$ are completely integrable and have already been studied extensively, see for example [10] and [15]. Moreover, for $p < 5$ all solutions in $H^1(\mathbf{R})$ are global and bounded in time as a result of the Gagliardo-Nirenberg inequality. The choice $p = 5$ is the smallest power such that the existing conservation laws do not imply a bound in $H^1(\mathbf{R})$, uniform in time, for all $H^1$-solutions, and thus no global existence can be guaranteed. From this, blowup in finite time is suspected for $p \geq 5$ where $p = 5$ is the so-called critical power.

Here, we study blowup solutions of equation (1.1) for $p \geq 5$. More specifically, we assume that the solutions blow up at some blowup time $T < \infty$ where

$$\max_x |\phi(x,t)| \to \infty \text{ as } t \uparrow T,$$

with $|\phi(x,t)| < \infty$ for all $t < T, x \in \mathbf{R}$. Note that since the mass (1.3) is conserved, the $L^2$-norm remains bounded whereas the $L^\infty$-norm goes to infinity.

Blowup solutions can arise when a solitary wave becomes unstable, hence, the study of stability of solitary waves is a first step towards analysing blowup. For all $p \geq 2$, explicit solitary waves of the GKdV equation are known,

$$\phi(x,t;C,x_0) = \left(\frac{p+1}{2} C \operatorname{sech}^2\left(\frac{p-1}{2}\sqrt{C}(x - x_0 - Ct)\right)\right)^{\frac{1}{p-1}}, \qquad (1.4)$$

where $C > 0$ is the wave speed and $x_0$ a translation parameter. For $p = 2, 3, 4$, this family of solutions is known to be (asymptotically) stable with respect to perturbations, [16]. For $p \geq 5$, even weaker statements of stability, such are orbital stability, are known to be false, [6]. Thus, $p = 5$ is also the critical case for the stability of solitons. A first numerical approach to try and understand stability and instability of solitons was taken in [7]. The instability manifests itself in blowup in finite time; perturbations of solitary waves form a similarity structure which in turn blows up.

Then, in [8], a thorough numerical study was conducted to detect the exact structure of the blowup solutions. Moreover, an asymptotic statement (for $|x| \to \infty$) about the structure and its self-similar form was made. However, the structure of the solution close to the point where it blows up was not studied there.

Analytically, the $H^1$-instability of solitons for the supercritical case $p > 5$ was considered in [6], see also references therein, and [21] for the choice $p = 5$. Then, in [11], a large set of initial data was obtained that leads to instability of solitons for $p \geq 5$. There, it was expected that these solutions actually blow up. Thereafter, the same authors analysed the blowup of solutions in a series of articles for the critical case $p = 5$. In those articles, solutions in the energy space $H^1(\mathbf{R})$ are analysed. These works start with [14] where the existence of solutions that blow up in finite or infinite time in $H^1$ was proved for $p = 5$. Then, in [12] an upper bound on the blowup rate was established. Moreover, a restriction on initial conditions such that blowup in finite time occurs was determined there. Finally, in [13] the question of the blowup profile, i.e. the asymptotic form of the solutions after rescaling, was studied. There, the authors prove that, for certain initial data, the solution converges at the blowup time $T$, to a self-similar travelling solution with a universal profile that is locally in space.

So far, the complete picture of the blowup solutions, for all $x$, has not yet been studied. In this article, we study blowup structures for $p \geq 5$ both by using numerical simulations and asymptotic analysis. In the asymptotic analysis, we finally resolve the overall structure of the solutions (for all $x$). We use the results of the numerical simulations to obtain an idea of the behaviour of the solution; this behaviour is then put into the equation in the form of a rescaling.

In figure 1, the result of a numerical simulation for $p = 6$ is given, see section 2 for more details and more results. In this figure, the time-frame where the peak of the solution shoots off to infinity is removed to show the dynamics of the solution as time increases towards the blowup time. See figure 3 for a plot where the solution that blows up is included, again for $p = 6$ and the same initial condition. As time increases, the solution moves to the right and the height of the bump grows. In this process, the width of the peak narrows and the solution blows up in finite time. It seems that the solution possesses a self-similar structure, note however, that the solution does not stay symmetric: the decay on the right-hand side of the bump is much faster compared to that on the left-hand side of the bump. Moreover, it can be observed that the speed with which the solution travels increases with time. More results are shown in section 2, where numerical simulations for various values of $p$ and different initial conditions are given.

Following the numerical simulations, we perform an asymptotic analysis to construct solutions of the GKdV equation (1.1) that blow up in finite time for $p \geq 5$. A so-called

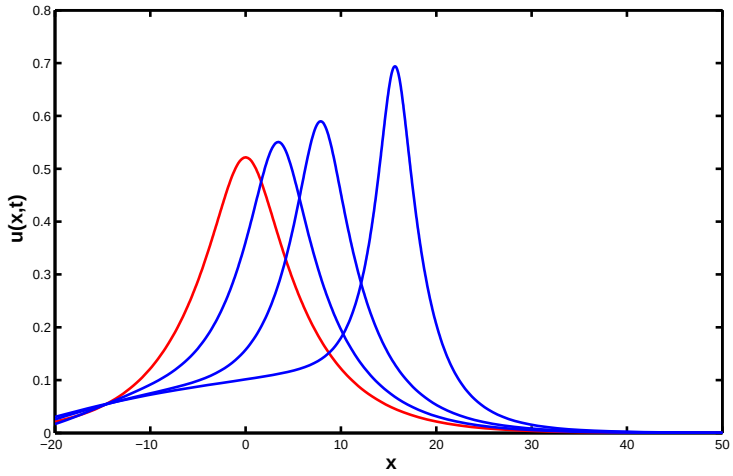


Figure 1: The solution as found in the numerical simulations for the GKdV for $p = 6$, $\tilde{C} = 1.02$ and $C = 0.03$, see for more details section 2. The initial condition (in red) and the solution at several equidistant time-steps is given. The solution travels to the right as time increases, and then, the solitary wave becomes unstable and blows up. Here, the final solution that blows up is removed, see figure 3 for a plot that includes the solution that shoots off to infinity.

dynamical rescaling is introduced in section 3 to scale the blowup out of the equation. This rescaling is based on the observations from the numerics. To analyse blowup solutions, we assume that $\phi = L(t)^{-\alpha} v$, $\alpha > 0$, where $v$ remains bounded and $L(t)$ goes to zero as $t \uparrow T$. Moreover, we define a new spatial variable $\xi$ that incorporates the self-similar narrowing of the peak as it travels where the fact that the speed of the solution depends on time is also incorporated, see section 3 expression (3.1) for the exact definition. This rescaling reduces equation (1.1) to the third-order partial differential equation

$$v_{\xi\xi\xi} + (v^p)_\xi - c(\beta - \gamma) v_\xi + L(t)^\gamma \beta \left[ \frac{2}{p-1} v + \xi v_\xi \right] + L(t)^{3\beta} v_t = 0, \tag{1.5}$$

where $L(t) \to 0$ as $t \uparrow T$ and $\beta$ and $\gamma$ are some unknown constants. Moreover, the $\mathcal{O}(1)$-parameter $c$ is related to the speed of the travelling wave. Now, the function $v(\xi, t)$ is assumed to be bounded with a maximum at $\xi = 0$, this means that the corresponding solution $\phi(\xi, t)$ of (1.1) blows up.

We will study equation (1.5) as the solution $\phi$ blows up, and hence, as $t \uparrow T$. Then, it turns out that the last term in this equation is much smaller than the other terms, and we can use asymptotic analysis to study equation (1.5) for $L \ll 1$. Mores pecifically, we apply asymptotic methods to construct bounded solutions, with a maximum at $\xi = 0$, that satisfy (1.5) together with the boundary conditions

$$|v| \to 0 \text{ as } t \to \pm\infty.$$

We analyse equation (1.5) in various regions of the $\xi$-axis , and thereafter, we match the solutions in these different regions to each other. We define a so-called bump region,

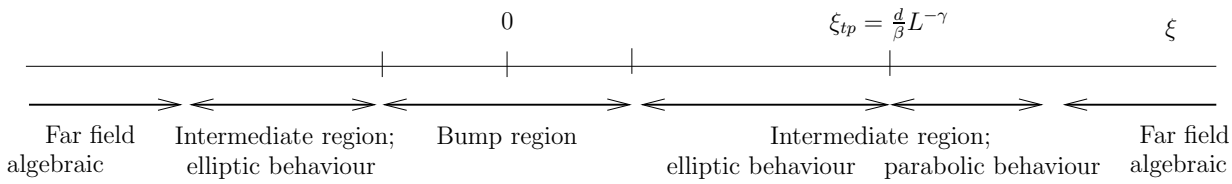


Figure 2: Different regions on the $\xi$-axis. As explained in the Introduction, solutions are studied in these different regions by using asymptotic analysis, and thereafter the solutions are matched.

where the maximum of the solution occurs at $\xi = 0$, and the far field for $\xi$ large, see figure 2. In the bump region, we find pulse-like, exponentially decaying, behaviour (hence the name of the region) under the condition that $c(\beta - \gamma) > 0$, see section 4. The solution in the far field, where $|\xi| \gg 1$ and $|v| \ll 1$, is analysed in section 4.1 and it turns out to be algebraically decaying. Since the solutions in the bump region are exponentially decaying and the solutions in the far field decay algebraically, the two regions cannot be matched together directly, and therefore, an intermediate region needs to be introduced. In the intermediate region, the corresponding equation has a turning point at $\xi_{tp} = \frac{d}{\beta}L^{-\gamma}$. At this point the behaviour of the solution changes from elliptic to parabolic. For all values of $p$, solutions to this equation are determined in section 4.2.

In section 5, the solution in the bump region is matched with the solution in the far field. To the left-hand side of the bump region, the solutions in the bump region and the far field are matched to each other by using the elliptic structure of the solutions in the intermediate region. To the right-hand side of the bump region, the solution in the bump region is matched to the elliptic solution whereas the solution in the far field is matched to the parabolic solution in the intermediate region.

Finally, in section 5.3 we summarise the results and give the resulting structure of the solution. It turns out that, unfortunately, the matching can only be done for $p = 5$. We have the idea that in order to perform the analysis for $p > 5$, the solution to the left-hand side of the bump has to be studied in more detail, see section 5.3 for a discussion. Also, improving the numerical simulations could turn out to be very valuable for this.

# 2 Numerical Simulations

In this section, we perform numerical simulations of solutions for equation (1.1) for various values of $p$ and different initial conditions. For the simulations an adaptive grid method is used, see [19]. We are interested in solutions that blowup in finite time, and therefore, we modify solution (1.4) slightly to obtain an initial condition for which blowup arises. Therefore, as an initial condition we take

$$\phi(x,0) = \tilde{C}\phi(x,0;0.03,0) = \tilde{C}\left[\left(\frac{0.03(p+1)}{2}\right)\operatorname{sech}^2\left(\frac{p-1}{2}\sqrt{0.03}x\right)\right]^{\frac{1}{p-1}}, \qquad (2.1)$$

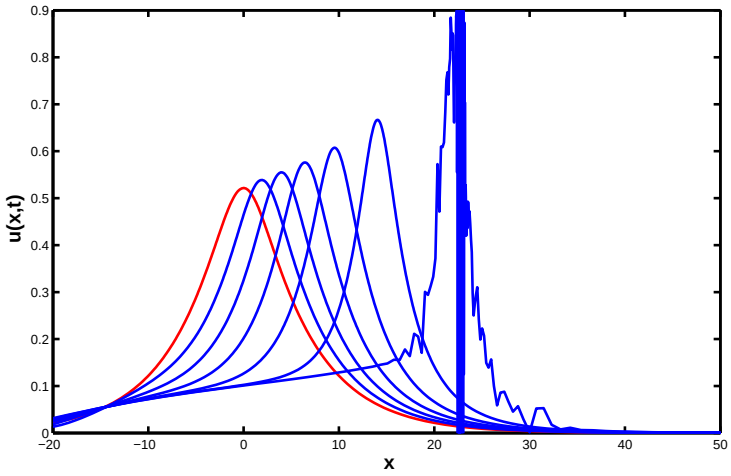


Figure 3: Solutions as found in the numerical simulations for the GKdV for $p = 6$, $\tilde{C} = 1.02, C = 0.03$. The initial condition (in red) and solutions at several equidistant time-steps are given. The solution travels to the right as time increases, and finally, the solitary wave becomes unstable and blows up. Here, the solution that blows up is also plotted; figure 1 gives the result of the same numeric simulation where this last solution is not given.

with $\tilde{C}$ a constant that is varied in the different simulations. This constant $\tilde{C}$ has to be chosen in a suitable way such that it satisfies the condition for blowup as found in [12], see the Introduction. In the numerics, the initial solution is iterated forward in time and equidistant time-plots are given in figure 1 for $p = 6$ and in figure 4 for $p = 5$(a.), $p = 7$(c.), $p = 8$(d.) where the initial condition is given in red and the value of $\tilde{C}$ is given in the caption. In these figures, the final solution that blows up is removed to show the dynamics of the solution as time increases towards the blowup time. The results of the simulations including the final blowup solution is given in figure 3 for $p = 6$. Then, in figure 4b. we only give the profile that is found just *before* the solution blows up for $p = 6$.

In the simulations, we find that the maximum of the initial condition starts to grow and finally blows up. Simultaneously, the solution travels to the right as time increases. Moreover, we conclude that since we plot equidistant solutions and the distance between the peaks increases, the speed at which the solution travels increases as time grows. In the process, the solution becomes asymmetric; to the right of the peak it decays to zero fast whereas to the left of the bump the decay is towards some kind of 'plateau' – it seems to become flat. We will find similar asymmetric behaviour of the solution that we construct asymptotically. However, it should be noted that the asymptotic solution is studied in new rescaled variables that will be introduced in section 3 – for which the solution remains bounded to leading order – and the plots given here are for the solution of the GKdV (1.1) that blows up.

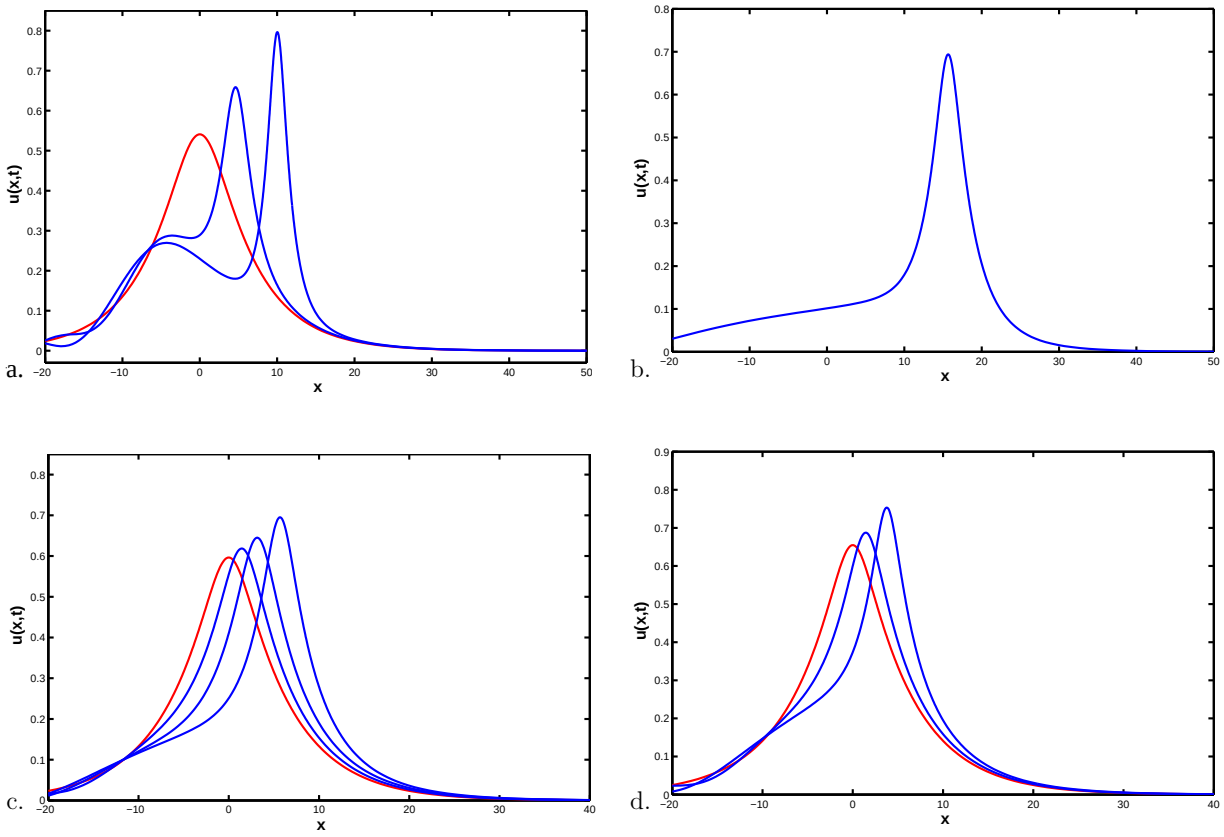


Figure 4: Solutions as found in the numerical simulations for the GKdV for a. $p = 5, \tilde{C} = 1.3$, b. $p = 6$, $\tilde{C} = 1.02$, c. $p = 7$, $\tilde{C} = 1.02$ and d. $p = 8$, $\tilde{C} = 1.02$. In all the plots we choose $C = 0.03$. In a., c. and d. the initial condition (in red) and solutions at several equidistant time-steps are given. In b. we only give the solution that is found just before the solution blows up.

# 3 Dynamical rescaling

In this section, we introduce a dynamical rescaling into the GKdV (1.1) such that the resulting equation does not exhibit blowup behaviour. For this, we rescale space, time and $\phi$ by factors that depend on a norm of the solution that blows up at the singularity. As a consequence, the rescaled problem no longer exhibits singular behaviour, and the norm of the rescaled solution remains bounded in time. Appropriate initial and asymptotic conditions guarantee that the solution of the original problem blows up.

The rescaled variables will be modelled to reflect the properties of the solution found in the numerical simulations in section 2. There, we observe that the peak of the solution narrows as time increases, and simultaneously, it travels with a speed that depends on time. We incorporate this behaviour in the dynamical rescaling, and therefore, introduce

$$\phi(x,t) = \frac{1}{L(t)^{\alpha}} v(\xi,t), \;\; \xi = \frac{1}{L(t)^{\beta}} \left( x - x_0 + cL(t)^{\beta-\gamma} \right), \tag{3.1}$$

where $L(t) \to 0$ as $t \to T$ and $\alpha, \beta$ and $\gamma$ positive constants. Here, the constant $c$ is related

to the speed and direction of the wave. The constant $x_0$ is a translation parameter that fixes the position of the blowup. Substituting the rescaling into equation (1.1) results, after multiplying with $L^{\alpha+3\beta}$, in

$$v_{\xi\xi\xi} + \frac{1}{L^{(p-1)\alpha-2\beta}}(v^p)_\xi - \frac{dL}{dt}L^{3\beta-\gamma-1}[-c(\beta-\gamma)v_\xi + L^\gamma(\alpha v + \beta\xi v_\xi)] + L^{3\beta}v_t = 0. \quad (3.2)$$

Now, we study this equation as $t \to T$, and therefore, $L$ is small. A significance degeneration is obtained when balancing the first with the second and the third term, then the other terms are higher-order terms in $L$ since $L \ll 1$. Balancing the third-order derivative with the non-linear term gives the relation

$$\alpha = \frac{2\beta}{p-1},$$

and a balance with the third term is obtained by setting

$$\frac{dL}{dt}L(t)^{3\beta-\gamma-1} = -1. \quad (3.3)$$

Here the sign is chosen such that $L(t)$ indeed decreases as $t$ approaches the blowup time. We can determine $L$ explicitly by solving relation (3.3) as

$$L(t) = ((3\beta-\gamma)(T-t))^{\frac{1}{3\beta-\gamma}}.$$

In order to guarantee that $L(t) \to 0$ as $t \uparrow T$, we need to choose

$$3\beta - \gamma > 0. \quad (3.4)$$

With these choices equation (3.2) becomes

$$v_{\xi\xi\xi} + (v^p)_\xi - c(\beta-\gamma)v_\xi + L^\gamma\beta\left[\frac{2}{p-1}v + \xi v_\xi\right] + L^{3\beta}v_t = 0. \quad (3.5)$$

It is this rescaled equation that is used in the asymptotic analysis where $v$ is assumed to be bounded. Now, a new challenge arises because of the fact that the $v$-equation still depends on time. However, since we analyse the equation as $t$ approaches to $T$, $L$ is small, and hence, the last term in the equation is small compared to the rest of the terms. Moreover, the $\mathcal{O}(L^\gamma)$-term is small as long as $\xi \ll L^{-\gamma}$. We analyse the solution in this region separately and where we denote it 'bump region' (since the bump of the solution is located there). As long as $\xi \ll L^{-\gamma}$, the leading order of the $v$-equation does not depend on time, and we can assume that the leading order of the solution does not depend on time, and hence, not on $L$. Outside this region, we do take the $\mathcal{O}(L^\gamma)$-term into account, see [5] for a similar approach.

In the next sections, we analyse the solution to equation (3.5) in different regions of the $\xi$-axis where we use that $L \ll 1$.

# 4 The bump region

In this section we study equation (3.5) in the region around $\xi = 0$. We assume that the solution has a maximum at $\xi = 0$, and thus, the condition

$$\frac{\partial v}{\partial \xi}|_{\xi=0} = 0$$

must hold.

As a first step, equation (3.5) is integrated with respect to $\xi$, resulting in

$$v_{\xi\xi} + v^p - dv + \mathcal{C} + L^\gamma \beta \left[ \xi v + \frac{3-p}{p-1} \int^\xi v ds \right] + L^{3\beta} \int^\xi v_t ds = 0, \tag{4.1}$$

where $\mathcal{C}$ is an integration constant and for notational convenience we introduce

$$d = c(\beta - \gamma).$$

To analyse equation (4.1) we use a regular asymptotic expansion

$$v = v_0 + L^\gamma v_1 + \text{h.o.t.} \tag{4.2}$$

Note that in the dynamical rescaling, in section 3, we assumed that $3\beta > \gamma$, (3.4). Therefore, $L^{3\beta} \ll L^\gamma$, and hence, this is the correct leading order term.

Substituting this expansion into (4.1) we collect the terms of $\mathcal{O}(1)$ under the assumption that $L^\gamma \xi \ll 1$. Then, the equation for $v_0$ reads

$$v_{0,\xi\xi} - dv_0 + v_0^p + \mathcal{C} = 0. \tag{4.3}$$

From the restriction on $\xi$ we find that (4.3) is the leading order equation as long as $|\xi| \ll L^{-\gamma}$. We call this the bump region since the peak of the solution lies in this region, see also figure 2. We are looking for solutions for which both the solution and $v_{\xi\xi}$ decay to zero as $|\xi| \to \infty$. Using these properties in equation (4.3) implies that $\mathcal{C} = 0$.

A bounded solution of (4.3) only exists for $d > 0$ and it is given by

$$v_0(\xi) = \left( \frac{d(p+1)}{2} \right)^{\frac{1}{p-1}} \operatorname{sech}^{\frac{2}{p-1}} \left( \frac{p-1}{2} \sqrt{d} \xi \right). \tag{4.4}$$

Note that there is a similarity between this solution and the solitary wave solution of the GKdV as given in (1.4) in the Introduction. However, the solution (1.4) is bounded whereas this solution (4.4) results, together with the dynamical rescaling (3.1), in a solution that blows up in finite time.

The condition $d > 0$ implies, with $d = c(\beta - \gamma)$, that $c$ and $\beta - \gamma$ must have the same sign. Note that this indeed corresponds to what was found in the numerical simulations performed in section 2. There, it is observed that the solution moves to the right which implies that $c$ has to be negative. Moreover, in the numerics the speed increases as $t$ approaches the blowup time. Hence, in the new rescaled variable $\xi$, the contribution of

$cL^{\beta-\gamma}$ should increase as $t \uparrow T$. This implies that $\beta < \gamma$, and thus, $\beta-\gamma$ and $c$ indeed have the same sign in the numerical simulations. However, the choice $\beta < \gamma$ is not necessary in our analysis, we only need that $d = c(\beta - \gamma) > 0$. In other words, the case $\beta > \gamma$ is still included here, although our numerics suggest the other choice.

Now we collect the $\mathcal{O}(L^\gamma)$-terms in the equation, this leads to the following equation for $v_1$

$$v_{1,\xi\xi} - dv_1 + pv_0^{p-1}v_1 = -\beta\left[\frac{3-p}{p-1}\int^\xi v_0 ds + \xi v_0\right] := g(\xi). \tag{4.5}$$

Using the expression for $v_0$, the function $g(\xi)$ can be determined explicitly as

$$\begin{aligned} g(\xi) &= -\beta\frac{2(3-p)}{\sqrt{d}(p-1)^2}\left(\frac{d(p+1)}{2}\right)^{\frac{1}{p-1}}\sinh\left(\frac{p-1}{2}\sqrt{d}\xi\right){}_2F_1\left[\frac{1}{2},\frac{p+1}{2(p-1)},\frac{3}{2},-\sinh^2\left(\frac{p-1}{2}\sqrt{d}\xi\right)\right] \\ &\quad -\beta\xi\left(\frac{d(p+1)}{2}\right)^{\frac{1}{p-1}}\operatorname{sech}^{\frac{2}{p-1}}\left(\frac{p-1}{2}\sqrt{d}\xi\right), \end{aligned} \tag{4.6}$$

where ${}_2F_1[a,b,c,z]$ denotes the (generalised) hypergeometric function.

We first study the homogeneous equation

$$v_{1_{\xi\xi}} - dv_1 + pv_0^{p-1}v_1 = 0. \tag{4.7}$$

One solution of this equation is given by

$$\psi_1(\xi) = v_{0,\xi} \tag{4.8}$$

$$= -\sqrt{d}\left(\frac{d(p+1)}{2}\right)^{\frac{1}{p-1}}\operatorname{sech}^{\frac{1+p}{p-1}}\left(\frac{(p-1)\sqrt{d}}{2}\xi\right)\sinh\left(\frac{(p-1)\sqrt{d}}{2}\xi\right), \tag{4.9}$$

which is odd and exponentially decaying. Using the method of reduction of order, a second linear independent solution can be found. We determine it explicitly as

$$\psi_2(\xi) = \psi_1(\xi)\int^\xi \frac{ds}{(v_{0,s})^2} \tag{4.10}$$

$$\begin{aligned} &= \left\{-\frac{3+p}{p-1}\sinh^2\left(\frac{p-1}{2}\sqrt{d}\xi\right)\operatorname{sech}^{\frac{p+1}{p-1}}\left(\frac{p-1}{2}\sqrt{d}\xi\right){}_2F_1\left[\frac{1}{2},\frac{p-5}{2(p-1)},\frac{3}{2},-\sinh^2\left(\frac{p-1}{2}\sqrt{d}\xi\right)\right]\right. \\ &\quad \left.+\cosh^{\frac{2}{p-1}}\left(\frac{p-1}{2}\sqrt{d}\xi\right)\right\}\frac{2}{d(p-1)}\left(\frac{d(p+1)}{2}\right)^{-\frac{1}{p-1}}. \end{aligned} \tag{4.11}$$

This solution is even and exponentially growing. Finally, the general solution of equation (4.5) is constructed by using the method of variation of parameters. This results in

$$v_1(\xi) = A_1\psi_1 + A_2\psi_2 - \psi_1\int^\xi \psi_2 g ds + \psi_2\int_0^\xi \psi_1 g ds, \tag{4.12}$$

where we use that the Wronski-determinant $\psi_1\frac{d\psi_2}{d\xi} - \frac{d\psi_1}{d\xi}\psi_2 = 1$. Here, the constants $A_1$ and $A_2$ are still free to choose.

Recall that we defined $\xi$ such that $v$ has a maximum at $\xi = 0$. This implies that we must choose $\frac{\partial v_1}{\partial \xi}|_{\xi=0} = 0$, and hence, $A_1 = 0$. The second constant $A_2$ will be determined in section 5.

In Appendix A, the integrals in solution $v_1$ (4.12) are evaluated for $\xi \gg 1$. The first term $\psi_1 \int^{\xi} \psi_2 g ds$ converges to a constant, and so does the integral $\int_0^{\xi} \psi_1 g ds$. This yields that

$$v_1 = \left(d^{2-p}(p+1)\right)^{\frac{1}{p-1}} 2^{\frac{p+2}{p-1}} e^{\sqrt{d}|\xi|} \left( -A_2 \left( \frac{d(p+1)}{2} \right)^{-\frac{2}{p-1}} + \frac{\sqrt{\pi}\beta(p-5)}{2\sqrt{d}(p-1)^2} \frac{\Gamma\left(\frac{2}{p-1}\right)}{\Gamma\left(\frac{p+3}{2(p-1)}\right)} \right) \quad (4.13)$$

as $\xi \to \infty$, and

$$\begin{aligned} v_1 = & \frac{1}{2d} \left( \frac{d(p+1)}{2} \right)^{\frac{1}{p-1}} \left[ 2 \frac{\sqrt{\pi}\beta(p-3)}{\sqrt{d}(p-1)^2} \frac{\Gamma(\frac{1}{p-1})}{\Gamma(\frac{p+1}{2(p-1)})} \right. \\ & \left. -2^{-\frac{2}{p-1}} e^{\sqrt{d}|\xi|} \left( A_2 \left( \frac{d(p+1)}{2} \right)^{-\frac{2}{p-1}} + \frac{\sqrt{\pi}\beta(p-5)}{2\sqrt{d}(p-1)^2} \frac{\Gamma\left(\frac{2}{p-1}\right)}{\Gamma\left(\frac{p+3}{2(p-1)}\right)} \right) \right] \end{aligned} \quad (4.14)$$

as $\xi \to -\infty$. Hence, for large $|\xi|$, the solution $v_1$ grows exponentially, depending on the choices of the parameters.

Thus, since $v_1$ is exponentially growing and $v_0$ is exponentially decaying, certain restrictions need to hold. We namely need to certify that expansion (4.2) remains a correct asymptotic expansion in the bump region. For this we need that $L^{\gamma}|v_1| \ll |v_0|$ for all $\xi$ in the bump region. To guarantee this there are two possibilities. We can either choose the coefficients in the problem in such a way that $v_1$ decays to zero as $|\xi| \to \infty$ or we can redefine the bump region. When using this latter approach, we restrict to that part of the bump region where the expansion is asymptotic. For that we need that $L^{\gamma} e^{\sqrt{d}|\xi|} \ll e^{-\sqrt{d}|\xi|}$, and thus, we take the restricted bump region to be the values for which $|\xi| \ll \log L^{-\gamma}$. This approach is similar to that in [18] where it is used in an asymptotic analysis of solutions for the Ginzburg-Landau equation. It turns out that it is not possible to have all the terms in $v_1$ decay to zero; we will come to this and postpone this analysis to the matching procedure in section 5.

## 4.1 The far field

In this section, we study solutions of equation (3.5) in the far field, so for $|\xi| \gg 1$. The numerical simulations suggest that $|v| \ll 1$ in this region. Hence we linearise around $v = 0$. We analyse the region where $|\xi| \gg 1$ by introducing the rescaling

$$y = L^{\sigma}\xi.$$

This gives after linearising

$$L^{3\sigma} v_{yyy} - dL^{\sigma} v_y + L^{\gamma}\beta \left[ \frac{2}{p-1} v + y v_y \right] + L^{3\beta} v_t = 0. \quad (4.15)$$

If we now take $\sigma > \gamma$, so that $\xi \gg 1$, the equation reduces to leading order to

$$\frac{2}{p-1}v + yv_y = 0. \tag{4.16}$$

Hence, the solution in the far field is given by

$$v_{ff} = c_{ff} y^{-\frac{2}{p-1}} = C_{ff}\xi^{-\frac{2}{p-1}}. \tag{4.17}$$

Note that the constant $C_{ff}$ can still depend on $L$.

We denote the far field solution for $\xi < 0$, hence, to the left of the bump region by

$$v_{ffleft} = C_{ff_{left}}\xi^{-\frac{2}{p-1}}, \tag{4.18}$$

and the far field solution for $\xi > 0$, to the right of the bump region, by

$$v_{ffright} = C_{ff_{right}}\xi^{-\frac{2}{p-1}}. \tag{4.19}$$

These solutions decay algebraically while the solution in the bump region has exponentially decay, consequently we can not match the two solutions directly. To overcome this problem, we introduce in the next section an intermediate region where we can match these solutions.

## 4.2 The intermediate region

In this section we introduce an intermediate region in which we analyse the solutions of equation (3.5). By setting $\sigma = \frac{1}{3}\gamma$ in equation (4.15) we obtain that to leading order

$$v_{yyy} + \frac{2\beta}{p-1}v + \left(\beta y - dL^{-\frac{2}{3}\gamma}\right)v_y = 0. \tag{4.20}$$

To write this equation in a more convenient form, we introduce the rescaling

$$z = -\left(\frac{\beta}{4}\right)^{\frac{1}{3}}\left(y - \frac{d}{\beta}L^{-\frac{2\gamma}{3}}\right),$$

which yields

$$v_{zzz} - 4zv_z - \frac{8}{p-1}v = 0. \tag{4.21}$$

This equation has a turning point at $z = 0$, which corresponds to

$$y = \frac{d}{\beta}L^{-\frac{2}{3}\gamma}, \text{ and hence, to } \xi_{tp} = \frac{d}{\beta}L^{-\gamma}.$$

Note that $\xi_{tp} > 0$, since $d, \beta > 0$. At the turning point, the behaviour of the solution changes from elliptic, on the left-hand side, to parabolic on the right-hand side. A general

solution of equation (4.21) can be found by using the method of Laplace, see also [20], by setting

$$v(z) = \int_C e^{zt} g(t) dt, \tag{4.22}$$

where $g(t)$ is a function that still has to be determined and $C$ is a path in the complex plane that can be determined once $g(t)$ is known. Substitution into equation (4.21) and integration by parts the equation becomes

$$\int_C e^{zt} \left[ g(t) \left( t^3 + \frac{4(p-3)}{p-1} \right) + 4t \frac{dg}{dt} \right] dt = 0, \tag{4.23}$$

with the boundary condition that

$$g(t) t e^{zt} = 0 \text{ on the boundary of the path } C. \tag{4.24}$$

Hence, we need to solve the first-order differential equation

$$g(t) \left( t^3 + \frac{4(p-3)}{p-1} \right) + 4t \frac{dg}{dt} = 0$$

together with the boundary condition (4.24). Solving this equation leads to

$$g(t) = D e^{\frac{-t^3}{12}} t^{\frac{3-p}{p-1}},$$

where $D$ is a constant. Thus, the integrand in (4.22) becomes

$$w(t) = e^{zt} g(t) = D e^{zt - \frac{1}{12} t^3} t^{\frac{3-p}{p-1}}. \tag{4.25}$$

The obvious choice for the path of integration, $C$, is a closed curve. However, since (4.25) is an entire function, this would give the trivial solution as a solution to equation (4.21). On the other hand for an open path with finite endpoints condition (4.24) is violated. Hence, the endpoints of the contour, that we denote by $a$ and $b$, must lie in the complex $\infty$-plane. When we set $t = re^{i\theta}$, the expression (4.25) $w(t)$ reduces for $t$ large, and hence $r$ large to

$$|w(t)| = r^{\frac{3-p}{p-1}} e^{rz\cos(\theta) - \frac{1}{12} r^3 \cos(3\theta)}. \tag{4.26}$$

In order to satisfy the boundary condition (4.24), we need that $tw(t) \to 0$ holds for $t \to a, b$. This can be achieved as long as $\cos(3\theta) > 0$. It is convenient to choose $\cos(3\theta) = 1$, which implies $\theta = 0, \frac{2\pi}{3}, \frac{4\pi}{3}$, and simultaneously let $r \to \infty$. This choice corresponds to the paths, $C_i$, shown in figure 5a. Summarising, we constructed three linearly independent solutions of (4.21) given by expression (4.22) where the contour $C$ is one of these paths of integration $C_i$.

In Appendix B, the asymptotic expansions of the corresponding solutions are determined, for $z \to \pm\infty$. For convenience, the paths in figure 5a are split up into the paths sketched in figure 5b. Thus, we take linear combinations of the solutions that were found before and for these determine the asymptotic expressions.

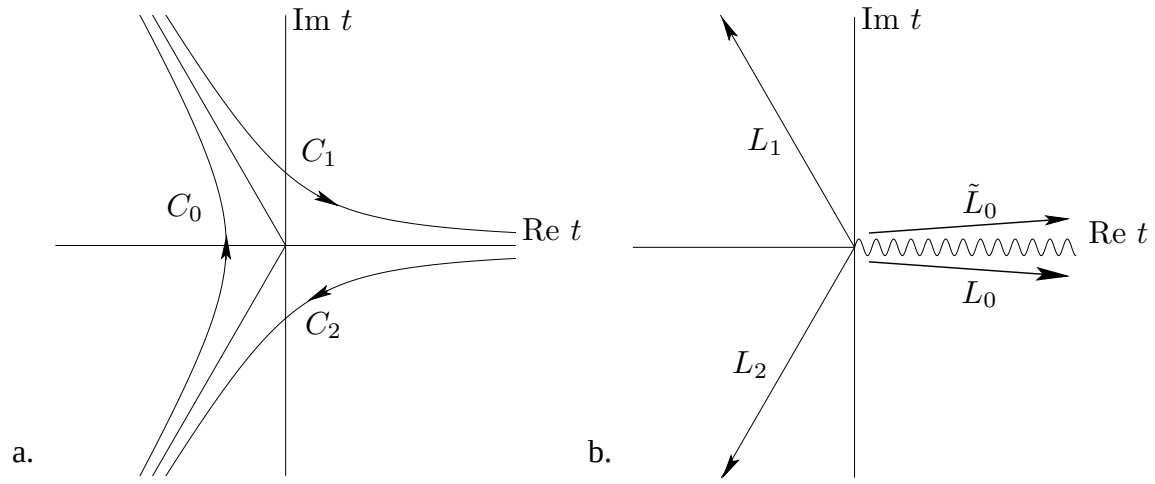


Figure 5: a. The paths of integration $C_i$, and b. the paths $L_i$. The curve $C_0$ converges to the paths $L_1$ and $L_2$. These paths $L_1$ and $L_2$ are straight lines that make an angle of $\theta = \frac{2\pi}{3}$ and $\theta = \frac{4\pi}{3}$, respectively, with the real positive axis.

Now, the solution to equation (4.21) to the right of the bump region, for $\xi < 0$, is given by

$$v_{IMright} = \sum_{i=0}^{2} c_i I_i(z), \tag{4.27}$$

where

$$I_i(z) = \int_{\Gamma_i} t^{\frac{3-p}{p-1}} e^{zt - \frac{1}{12}t^3} dt, \tag{4.28}$$

and the solution to the left of the bump region, by

$$v_{IMleft} = \sum_{i=0}^{2} d_i I_i, \tag{4.29}$$

where $c_i, d_i$ are constants. Here, we choose the paths $\Gamma_i$ as follows

$$\begin{array}{rcl} \Gamma_0 & = & C_0, \\ \Gamma_1 & = & \tilde{L}_0, \\ \Gamma_2 & = & L_1 + L_2. \end{array} \tag{4.30}$$

For $p = 5$, equation (4.21) reduces to

$$v_{zzz} - 4zv_z - 2v = 0. \tag{4.31}$$

Then, solutions are explicitly known, see expression [10.4.57] in [2] and they are given by products of the Airy functions, $A_i$ and $B_i$, hence by $A_i^2, B_i^2$ and $A_i B_i$. The contours $\Gamma_i$ are chosen such that the following relations hold between these products of Airy functions

and the solutions $I_i$ (4.28), see [17]

$$\begin{aligned} A_i^2 &= \frac{1}{4\pi^{\frac{3}{2}}} I_0 \\ A_i B_i &= \frac{1}{4\pi^{\frac{3}{2}}} I_2 \\ B_i^2 &= \frac{1}{\pi^{\frac{3}{2}}} I_1 - A_i^2. \end{aligned}$$

# 5 Matching

In this section, we match the solution in the bump region to the solutions in the far field. We do this by first matching the right-hand side of the bump solution with the solution in the intermediate region and then match that solution to the far field solution. In section 5.2 we perform a similar procedure to the left of the bump region.

## 5.1 Matching the solutions to the right of the bump region

Here we match the solutions to the right of the bump region, hence for $\xi > 0$. We start with matching the solution in the intermediate region to the solution in the far field, (4.19), for $\xi \gg \xi_{tp}$, $z < 0$. Moreover, we assume that $\xi$ satisfies $L^{\frac{\gamma}{3}}(\xi_{tp} - \xi) \gg 1$, and $|z| \gg 1$, such that the asymptotic expansion for the solutions as determined in Appendix B in the intermediate region can be used. Then, by using (B.10), (B.12) and (B.13) in Appendix B, the asymptotic expansions of the solutions in the intermediate region are given by

$$\begin{aligned} v_{IMright} &= c_0 I_0 + c_1 I_1 + c_2 I_2 \\ &= \left( 2ic_0(-1)^{\frac{3-p}{p-1}} \cos\left(\tfrac{\pi(5-p)}{2(p-1)}\right) + c_1 + 2c_2(-1)^{\frac{-2}{p-1}} \cos\left(\tfrac{(p-3)\pi}{p-1}\right) \right) \Gamma(\tfrac{2}{p-1}) \left(\tfrac{\beta}{4} L^{\gamma}\right)^{-\frac{2}{3(p-1)}} \xi^{-\frac{2}{p-1}} \end{aligned} \tag{5.1}$$

for $p > 5$.

For convenience and in order to make sure that $v$ is real, we introduce

$$C_0 = ic_0(-1)^{\frac{3-p}{p-1}} \text{ and } C_2 = c_2(-1)^{\frac{-2}{p-1}},$$

which are both assumed to be real. This choice guarantees that the solution remains real for all $\xi$.

Note that for $p = 5$ the asymptotic expression for the solution is different, namely

$$\begin{aligned} v_{IMright} &= \left( -2c_0 + c_1 + 2c_0 \cos\left( \frac{2}{3}(L\beta)^{\frac{1}{2}}(\xi - \frac{d}{\beta} L^{-\gamma})^{\frac{3}{2}} - \frac{\pi}{2} \right) \right. \\ &\quad \left. + 2c_2 i \cos\left( \frac{2}{3}(L\beta)^{\frac{1}{2}}(\xi - \frac{d}{\beta} L^{-\gamma})^{\frac{3}{2}} \right) \right) \sqrt{\pi} \left( \frac{\beta}{4} L^{\gamma} \right)^{-\frac{1}{6}} \xi^{-\frac{1}{2}}. \end{aligned} \tag{5.2}$$

We first do the matching for $p > 5$ and then come back to the case $p = 5$.

The solution in the far field is given by

$$v_{ff_{right}} = C_{ff_{right}} \xi^{-\frac{2}{p-1}}, \tag{5.3}$$

so by choosing, for $p > 5$,

$$C_{ff_{right}} = \left( 2C_0 \cos\left(\frac{\pi(5-p)}{2(p-1)}\right) + c_1 + 2C_2 \cos\left(\frac{(p-3)\pi}{p-1}\right)\right) \Gamma\left((\frac{2}{p-1}\right) \left(\frac{\beta}{4} L^\gamma\right)^{-\frac{2}{3(p-1)}}, \tag{5.4}$$

the two solutions are perfectly matched.

Now, we match the bump solution, (4.2), to the solution, (4.27), valid to the right-hand side of the bump region and to the left-hand side of the turning point. The leading order term for $\xi \ll \xi_{tp}$, is given by

$$\begin{aligned} v_{IMright} \quad =& C_0 2^{\frac{5-p}{2(p-1)}} d^{\frac{1}{p-1}-\frac{3}{4}} \left(\frac{\beta L^\gamma}{2}\right)^{\frac{3p-7}{6(p-1)}} e^{-\frac{2}{3}\beta^{-1} d^{\frac{3}{2}} L^{-\gamma} + \sqrt{d}\xi} \\ &+ c_1 2^{\frac{5-p}{2(p-1)}} d^{\frac{1}{p-1}-\frac{3}{4}} \left(\frac{\beta L^\gamma}{2}\right)^{\frac{3p-7}{6(p-1)}} e^{\frac{2}{3}\beta^{-1} d^{\frac{3}{2}} L^{-\gamma} - \sqrt{d}\xi} - 2C_2 d^{\frac{-2}{p-1}} \left(\frac{\beta L^\gamma}{2}\right)^{\frac{4}{3(p-1)}} \Gamma\left(\frac{2}{p-1}\right). \end{aligned} \tag{5.5}$$

Using the expressions for $v_0$, (4.4), and for $v_1$, (4.13), the asymptotic behaviour of the solution in the bump region is given by

$$\begin{aligned} v(\xi) \quad =& \quad (2d(p+1)(p-1)^{\frac{1}{2}})^{\frac{1}{p-1}} e^{-\sqrt{d}\xi} \\ &+ L^\gamma \left(d^{2-p}(p+1)\right)^{\frac{1}{p-1}} 2^{\frac{p+2}{p-1}} e^{\sqrt{d}|\xi|} \left( -A_2 \left(\frac{d(p+1)}{2}\right)^{-\frac{2}{p-1}} + \frac{\sqrt{\pi}\beta(p-5)}{2\sqrt{d}(p-1)^2} \frac{\Gamma\left(\frac{2}{p-1}\right)}{\Gamma\left(\frac{p+3}{2(p-1)}\right)} \right), \end{aligned} \tag{5.6}$$

to leading order. Recall that to ensure that this expression remains an asymptotic expansion in the bump region, we can take two approaches, see for more details the discussion in section 4 after expression (4.14). For now, we leave the approach that will be taken open and return to this at the end of this section.

Both the first term in expression (5.6) and the second term in (5.5) are exponentially decaying, therefore, these two terms can be matched with each other. The last term in (5.5) is constant, hence, this should be matched to higher order terms in the bump leading (we do not do this here). Also, we match the exponentially growing terms in both expressions. Thus, we choose

$$c_1 \quad = 2^{\frac{p-5}{2(p-1)}} d^{\frac{3}{4}} \left(\frac{\beta L^\gamma}{2}\right)^{\frac{7-3p}{6(p-1)}} e^{-\frac{2}{3}\beta^{-1} d^{\frac{3}{2}} L^{-\gamma}} (2(p+1)(p-1)^{\frac{1}{2}})^{\frac{1}{p-1}}, \tag{5.7}$$

$$C_0 \quad = \quad 2^{-\frac{17}{3(p-1)}} d^{-\frac{1}{4}} \beta^{\frac{7-3p}{6(p-1)}} L^{\gamma\frac{3p+1}{6(p-1)}} e^{\frac{2}{3}\beta^{-1} d^{\frac{3}{2}} L^{-\gamma}} \left[ -A_2 \left(\frac{d(p+1)}{2}\right)^{-\frac{2}{p-1}} + \frac{\sqrt{\pi}\beta(p-5)}{2\sqrt{d}(p-1)^2} \frac{\Gamma\left(\frac{2}{p-1}\right)}{\Gamma\left(\frac{p+3}{2(p-1)}\right)} \right].$$

This choice for $C_0$, where it is exponentially large, implies that the constant $C_{ffright}$ also has to be exponentially large, and hence, this contradicts with the fact that we assume in section 4.1 that $|v| \ll 1$ in the far field. Hence, we need to choose $C_0 = 0$ and this also implies that

$$A_2 = \left(\frac{d(p+1)}{2}\right)^{\frac{2}{p-1}} \frac{\sqrt{\pi}\beta(p-5)}{2\sqrt{d}(p-1)^2} \frac{\Gamma\left(\frac{2}{p-1}\right)}{\Gamma\left(\frac{p+3}{2(p-1)}\right)}. \tag{5.8}$$

Now, we return to the case $p = 5$. To be able to match the solution in the intermediate region (5.2) to the far field solutions, solution (5.2) cannot be oscillating, and therefore we choose $c_0 = c_2 = 0$. Then, the solution in the intermediate region can be matched to the far field solution by choosing

$$C_{ff_{right}} = c_1\sqrt{\pi}\left(\frac{\beta}{4}L^{\gamma}\right)^{-\frac{1}{6}}. \tag{5.9}$$

The matching of the solution in the intermediate region to the bump solution goes in the same way as for $p > 5$ (with $C_2 = 0$). Hence, the constant $c_1$ is still given by expression (5.7) where $p = 5$ must be substituted.

## 5.2 Matching the solutions to the left of the bump region

In this section, the solutions for $\xi < 0$ will be matched. We start by matching the solution valid in the intermediate region, (4.29) with the solution valid in the far field, (4.18). For $|\xi| \gg L^{-\gamma}$, the asymptotic expansions of the various terms of solution (4.29) are given by

$$\begin{aligned} v_{IMleft} &= 2^{\frac{5-p}{2(p-1)}} d^{\frac{1}{p-1}-\frac{3}{4}} \left(\frac{\beta L^{\gamma}}{2}\right)^{\frac{3p-7}{6(p-1)}} \left(D_0 e^{-\frac{2}{3}\beta^{-1}d^{\frac{3}{2}}L^{-\gamma}-\sqrt{d}|\xi|}\right. \\ &\quad \left. + d_1 e^{\frac{2}{3}\beta^{-1}d^{\frac{3}{2}}L^{-\gamma}+\sqrt{d}|\xi|}\right) - 2D_2\left(\frac{\beta}{4}L^{\gamma}\right)^{\frac{-2}{3(p-1)}} |\xi|^{\frac{-2}{p-1}}\Gamma\left(\frac{2}{p-1}\right). \end{aligned} \tag{5.10}$$

Note that this is the leading order expression for all $p \leq 5$. Similar as before we introduce

$$D_0 = d_0 i(-1)^{\frac{3-p}{p-1}}, D_2 = d_2(-1)^{\frac{-2}{p-1}},$$

where $D_0$ and $D_2$ are assumed to be real, in order to make the expression for the solution real. Since the second term in (5.10) is exponentially growing, we must choose $d_1 = 0$, otherwise the solution cannot be matched to the far field solution.

The solution in the far field is given by

$$v_{ffleft} = C_{ffleft}|\xi|^{-\frac{2}{p-1}}. \tag{5.11}$$

Therefore, the far field solution, (4.18), is matched to the solution valid in the intermediate region, (4.29), by choosing

$$C_{ffleft} = -2D_2\left(\frac{\beta}{4}L^{-\gamma}\right)^{\frac{-2}{3(p-1)}}\Gamma\left(\frac{2}{p-1}\right). \tag{5.12}$$

Note that the first term in (5.10) is exponentially small and hence $D_0$ is still free to choose.

Next, we match the solution in the bump region, (4.2), with the solution in the intermediate region, (4.29). After setting $d_1 = 0$, the leading order of the various terms of the solution (4.29) is given by

$$\begin{aligned} v_{IMleft} &= D_0 2^{\frac{5-p}{2(p-1)}} d^{\frac{1}{p-1}-\frac{3}{4}} \left(\frac{\beta L^\gamma}{2}\right)^{\frac{3p-7}{6(p-1)}} e^{-\frac{2}{3}\beta^{-1}d^{\frac{3}{2}}L^{-\gamma}-\sqrt{d}|\xi|} \\ &\quad -2D_2 d^{\frac{-2}{p-1}} \left(\frac{\beta L^\gamma}{2}\right)^{\frac{4}{3(p-1)}} \Gamma\left(\frac{2}{p-1}\right). \end{aligned} \tag{5.13}$$

Evaluating expression (4.4) and using (4.14), the asymptotic behaviour of the solution in the bump region is given by

$$\begin{aligned} v_0(\xi) &= (2d(p+1)(p-1)^{\frac{1}{2}})^{\frac{1}{p-1}} e^{-\sqrt{d}|\xi|} + L^\gamma \frac{1}{2d}\left(\frac{d(p+1)}{2}\right)^{\frac{1}{p-1}} \left[2\frac{\sqrt{\pi}\beta(p-3)}{\sqrt{d}(p-1)^2}\frac{\Gamma\left(\frac{1}{p-1}\right)}{\Gamma\left(\frac{p+1}{2(p-1)}\right)}\right. \\ &\quad \left. -2^{-\frac{2}{p-1}} e^{\sqrt{d}|\xi|}\left(A_2\left(\frac{d(p+1)}{2}\right)^{-\frac{2}{p-1}} + \frac{\sqrt{\pi}\beta(p-5)}{2\sqrt{d}(p-1)^2}\frac{\Gamma\left(\frac{2}{p-1}\right)}{\Gamma\left(\frac{p+3}{2(p-1)}\right)}\right)\right]. \end{aligned} \tag{5.14}$$

Now, the exponentially growing $\mathcal{O}(L^\gamma)$-term in this expression can only be matched to an exponentially growing term in the intermediate region resulting in an exponentially growing term in the far field and this is not possible. Therefore, we must choose $A_2$ such that the last term in (5.14) vanishes, leading to

$$A_2 = -\left(\frac{d(p+1)}{2}\right)^{-\frac{2}{p-1}} \frac{\sqrt{\pi}\beta(p-5)}{2\sqrt{d}(p-1)^2}\frac{\Gamma\left(\frac{2}{p-1}\right)}{\Gamma\left(\frac{p+3}{2(p-1)}\right)}. \tag{5.15}$$

In order to match the bump solution (5.14) with expression (5.13) valid on the left-hand side of the bump region, we choose

$$\begin{aligned} D_0 &= 2^{\frac{3p-8}{3(p-1)}} d^{\frac{3}{4}} (\beta L^\gamma)^{\frac{7-3p}{6(p-1)}} ((p+1)(p-1)^{\frac{1}{2}})^{\frac{1}{p-1}} e^{\frac{2}{3}\beta^{-1}d^{\frac{3}{2}}L^{-\gamma}}, \\ D_2 &= -2^{\frac{4-3p}{3(p-1)}} d^{\frac{3(3-p)}{2(p-1)}} (\beta L^\gamma)^{\frac{3p-7}{3(p-1)}} (p+1)^{\frac{1}{p-1}} \frac{\sqrt{\pi}\beta(p-3)}{(p-1)^2}\frac{\Gamma\left(\frac{1}{p-1}\right)}{\Gamma\left(\frac{2}{p-1}\right)\Gamma\left(\frac{p+1}{2(p-1)}\right)}. \end{aligned}$$

and complete the matching procedure.

## 5.3 The constructed solution

Now, we summarise the results of the previous sections. Combining both expressions for $A_2$, (5.8) and (5.15), that were obtained in the above analysis we conclude that we must choose

$$A_2 = 0 \text{ and } p = 5.$$

Hence, the above asymptotic analysis can only be done in the case when $p = 5$. Then, we find that, in the analysis in section 5.1, we must take $C_2 = 0$ and $C_{ff_{right}}$ must satisfy (5.9). Note that this choice also implies that the exponentially growing terms that were found in the bump solution –coming from $v_1$ (4.12)– are no longer present. It follows from (4.13) that for $\xi > 0$, $v_1 \to 0$ as $\xi \to \infty$, and (4.14) implies that for $\xi < 0$, $v_1$ converges to a (nonzero) constant $v_{1_{left}}$ as $|\xi| \to \infty$.

Hence, the expansion for the bump solution still fails to be asymptotic for $\xi < 0$. One approach that could be taken to make the solution asymptotic is to choose the coefficients in the problem such that the constant $v_{1_{left}}$ is equal to zero. It turns out that this is not possible. Another approach to make the bump solution asymptotic, is to restrict to that the part of the negative $\xi$-values of the bump region where it is aymptotic. Indeed, if we restrict to the interval $\xi_1 < \xi < \xi_2$ where $\xi_1 < 0$, $|\xi_1| \ll \log L^{-\gamma}$ and still take $\xi_2 > 0$, $|\xi_2| \ll L^{-\gamma}$, we find an asymptotic expansion for the solution. Note that the assumptions made in the intermediate region still hold and, hence, our matching analysis is still valid. This approach was already suggested in section 4 and is similar to the approach taken in [18].

Now, we give a summary of the resulting asymptotic expressions for the solution in the various regions. In the following, $v_{bumpleft}$ and $v_{bumpright}$ are the asymptotic expressions for the solution in the bump region for $\xi < 0$ (with $|\xi| \ll \log L^{-\gamma}$), and $\xi > 0$ (with $|\xi| \ll \mathcal{O}(L^{\gamma})$), respectively, for $\xi$ large,

$$\begin{aligned}
v_{ffleft} &= C_{ff_{left}}|\xi|^{-\frac{1}{2}} = \sqrt{\pi}2^{-\frac{13}{6}}d^{-\frac{3}{4}}\beta^{\frac{3}{2}}L^{\frac{\gamma}{2}}3^{\frac{1}{4}}\frac{\Gamma(\frac{1}{4})}{\Gamma(\frac{3}{4})}|\xi|^{-\frac{1}{2}} \\
v_{bumpleft} &= (24d)^{\frac{1}{4}}e^{-\sqrt{d}|\xi|} + L^{\gamma}d^{-\frac{5}{4}}3^{\frac{1}{4}}\sqrt{\pi}\beta\frac{\Gamma(\frac{1}{4})}{8\Gamma(\frac{3}{4})} \\
v_{bumpright} &= (24d)^{\frac{1}{4}}e^{-\sqrt{d}\xi} \\
v_{ffright} &= C_{ff_{right}}\xi^{-\frac{1}{2}} = \sqrt{\pi}d^{\frac{3}{4}}\left(\beta L^{\gamma}\right)^{-\frac{1}{2}}2^{\frac{17}{12}}3^{\frac{1}{4}}e^{-\frac{2}{3}\beta^{-1}d^{\frac{3}{2}}L^{-\gamma}}\xi^{-\frac{1}{2}}.
\end{aligned}$$

Note that the constructed solution is **not** symmetric (around $\xi = 0$). The asymptotic solution decays exponentially to zero on the right-hand side of the bump whereas on the left-hand side of the bump the solution decays exponentially to some $\mathcal{O}(L^{\gamma})$-constant. A similar structure was observed in the numerical simulations presented in section 2, figure 4. Although one should recall that the constructed solution, $v$, as given above is written in terms of the dynamically rescaled variables (3.1) whereas in the numerics in figure 4 the blowup solution $\phi$ of equation (1.1) is given in the original variables $\phi, \xi$ and $t$.

As already mentioned previously, the construction in this article can unfortunately only be performed for $p = 5$. We think that for $p > 5$ the region to the left-hand side of the bump needs to be analysed in more detail since special behaviour is observed there. Moreover, improving the numerical simulations would be valuable in order to understand the structure of the solutions even better.

**Acknowledgements** The work of V.R. was partially supported by a VIDI-grant of the Dutch Science Organisation (NWO).

# A Appendix: the integrals in the bump region

In this Appendix, we determine the two integrals in the solution $v_1$, (4.12) in the bump region.

## A.1 First integral

Here, we determine the integral $\psi_2 \int_0^\xi \psi_1 g ds$, this can be done explicitly. Also, the asymptotic expression as $\xi \to \pm\infty$ is found. The integral $\int_0^\xi \psi_1 g ds$ is found by determining all separate terms in the integral explicitly

$$\begin{aligned}
\int_0^\xi \psi_1 g ds &= \int_0^\xi -\beta \frac{3-p}{p-1} v_{0,s} \int_0^s v_0 dr ds - \int_0^\xi \beta s v_0 v_{0,s} ds, \\
&= -\beta \frac{3-p}{p-1} \left[ v_0 \int_0^\xi v_0 ds - \int_0^\xi v_0^2 ds \right] \\
&\quad -\beta \left[ \frac{1}{2} \xi v_0^2 - \frac{1}{2} \int_0^\xi v_0^2 ds \right], \\
&= -\beta \left[ \frac{3-p}{p-1} v_0 \int_0^\xi v_0 ds + \frac{1}{2} \xi v_0 - \left( \frac{3-p}{p-1} + \frac{1}{2} \right) \int_0^\xi v_0^2 ds \right], \\
&= -\beta \left[ \frac{3-p}{p-1} v_0 \int_0^\xi v_0 ds + \frac{1}{2} \xi v_0^2 + \frac{p-5}{2(p-1)} \int_0^\xi v_0^2 ds \right].
\end{aligned}$$

Here

$$\begin{aligned}
v_0 \int_0^\xi v_0 ds &= \frac{2}{\sqrt{d}(p-1)} \left( \frac{d(p+1)}{2} \right)^{\frac{2}{p-1}} \operatorname{sech}^{\frac{2}{p-1}} \left( \frac{p-1}{2} \sqrt{d} \xi \right) \sinh \left( \frac{p-1}{2} \sqrt{d} \xi \right) \\
&\quad \times {}_2F_1 \left[ \frac{1}{2}, \frac{p+1}{2(p-1)}, \frac{3}{2}, -\sinh^2 \left( \frac{p-1}{2} \sqrt{d} \xi \right) \right], \\
&= \pm \frac{2}{\sqrt{d}(p-1)} \left( \frac{d(p+1)}{2} \right)^{\frac{2}{p-1}} \operatorname{sech}^{\frac{2}{p-1}} \left( \frac{p-1}{2} \sqrt{d} \xi \right) \frac{\Gamma(\frac{1}{p-1}) \Gamma(\frac{3}{2})}{\Gamma(\frac{p+1}{2(p-1)})} \\
&= \pm \frac{\sqrt{\pi}}{\sqrt{d}(p-1)} \left( d(p+1) \right)^{\frac{2}{p-1}} e^{-\sqrt{d}|\xi|} \frac{\Gamma(\frac{1}{p-1})}{\Gamma(\frac{p+1}{2(p-1)})} \\
\xi v_0^2 &= \left( \frac{d(p+1)}{2} \right)^{\frac{2}{p-1}} \xi \operatorname{sech}^{\frac{4}{p-1}} \left( \frac{p-1}{2} \sqrt{d} \xi \right) \; e^{-2\sqrt{d}|\xi|},
\end{aligned}$$

$$\begin{aligned}
\int_0^\xi v_0^2 &= \frac{2}{\sqrt{d}(p-1)} \left( \frac{d(p+1)}{2} \right)^{\frac{2}{p-1}} \sinh \left( \frac{p-1}{2} \sqrt{d} \xi \right) {}_2F_1 \left[ \frac{1}{2}, \frac{p+3}{2(p-1)}, \frac{3}{2}, -\sinh^2 \left( \frac{p-1}{2} \sqrt{d} \xi \right) \right] \\
&= \pm \frac{\sqrt{\pi}}{\sqrt{d}(p-1)} \left( \frac{d(p+1)}{2} \right)^{\frac{2}{p-1}} \frac{\Gamma(\frac{2}{p-1})}{\Gamma(\frac{p+3}{2(p-1)})}
\end{aligned}$$

Hence, the integral can be explicitly determined.

Now, we find the asymptotic behaviour for large $\xi$ by using the asymptotic expansion for the hyperbolic function ${}_2F_1$ (see for example [15.3] in [2]).

$$\begin{aligned} {}_2F_1[a,b,c,z] &= \frac{\Gamma(b-a)\Gamma(c)}{\Gamma(b)\Gamma(c-a)}(-z)^{-a}\left(1+\frac{a(1+a-c)}{(1+a-b)z}+\cdots\right) \\ &+ \frac{\Gamma(a-b)\Gamma(c)}{\Gamma(a)\Gamma(c-b)}(-z)^{-b}\left(1+\frac{b(1+b-c)}{(1-a+b)z}+\cdots\right), \end{aligned} \tag{A.1}$$

as $|z|\to\infty \wedge a-b\notin \mathbf{Z}$.

Therefore, as $\xi\to\pm\infty$, the asymptotics is given by

$$\begin{aligned} &\psi_2\left(A_2+\int_0^\xi \psi_1 g ds\right) \\ &= \frac{1}{2d}\left(\frac{d(p+1)}{2}\right)^{\frac{1}{p-1}}\left[2^{-\frac{2}{p-1}}e^{\sqrt{d}|\xi|}\left(-A_2\left(\frac{d(p+1)}{2}\right)^{-\frac{2}{p-1}}\pm\frac{\sqrt{\pi}\beta(p-5)}{2\sqrt{d}(p-1)^2}\frac{\Gamma\left(\frac{2}{p-1}\right)}{\Gamma\left(\frac{p+3}{2(p-1)}\right)}\right)\right. \\ &\left.\mp\frac{\sqrt{\pi}\beta(p-3)}{\sqrt{d}(p-1)^2}\frac{\Gamma(\frac{1}{p-1})}{\Gamma(\frac{p+1}{2(p-1)})}\right]+\mathcal{O}(e^{-\sqrt{d}|\xi|}) \end{aligned}$$

## A.2 Second integral

Now we analyse the second integral $\psi_1\int^\xi \psi_2 g ds$. As $\xi\to\pm\infty$, the asymptotics of the function $\psi_1$ (4.9) is given by

$$\psi_1(\xi)=\mp\sqrt{d}\left(\frac{d(p+1)}{2}\right)^{\frac{1}{p-1}}2^{\frac{2}{p-1}}e^{-\sqrt{d}|\xi|}. \tag{A.2}$$

Using expressions (4.11) and (4.6), the integral $\int^\xi \psi_2 g ds$ is given by

$$\begin{aligned} \int^\xi \psi_2 g ds &= \frac{4\beta(p-3)(p+3)}{d\sqrt{d}(p-1)^4}\int^\xi \sinh^3\left(\frac{p-1}{2}\sqrt{d}s\right)\operatorname{sech}^{1+\frac{2}{p-1}}\left(\frac{p-1}{2}\sqrt{d}s\right) \\ &\times {}_2F_1\left[\frac{1}{2},\frac{p-5}{2(p-1)},\frac{3}{2},-\sinh^2\left(\frac{p-1}{2}\sqrt{d}s\right)\right]{}_2F_1\left[\frac{1}{2},\frac{p+1}{2(p-1)},\frac{3}{2},-\sinh^2\left(\frac{p-1}{2}\sqrt{d}s\right)\right]ds \\ &-\frac{4\beta(p-3)}{d\sqrt{d}(p-1)^3}\int^\xi \cosh^{\frac{2}{p-1}}\left(\frac{p-1}{2}\sqrt{d}s\right)\sinh\left(\frac{p-1}{2}\sqrt{d}s\right) \\ &\times {}_2F_1\left[\frac{1}{2},\frac{p+1}{2(p-1)},\frac{3}{2},-\sinh^2\left(\frac{p-1}{2}\sqrt{d}s\right)\right]ds \\ &+\frac{2\beta(p+3)}{d(p-1)^2}\int^\xi s\sinh^2\left(\frac{p-1}{2}\sqrt{d}s\right)\operatorname{sech}^{1+\frac{4}{p-1}}\left(\frac{p-1}{2}\sqrt{d}s\right) \\ &\times {}_2F_1\left[\frac{1}{2},\frac{p-5}{2(p-1)},\frac{3}{2},-\sinh^2\left(\frac{p-1}{2}\sqrt{d}s\right)\right]ds \end{aligned}$$

$$
\begin{aligned}
& -\frac{2\beta}{d(p-1)}\int^{\xi} s ds \\
= \; & -\frac{4\beta(p-3)(p+3)}{d\sqrt{d}(p-1)^4}\int^{\xi} I ds + \frac{4\beta(p-3)}{d\sqrt{d}(p-1)^3}\int^{\xi} II ds \\
& +\frac{2\beta(p+3)}{d(p-1)^2}\int^{\xi} III ds - \frac{\beta\xi^2}{d(p-1)}
\end{aligned}
$$

Using the asymptotic expression (A.1), the asymptotic behaviour as $\xi \to \pm\infty$ of the integrands is determined. Then these expressions are integrated.

$$
\begin{aligned}
\frac{4\beta(p-3)(p+3)}{d\sqrt{d}(p-1)^4}\lim_{\xi\to\pm\infty}\int^{\xi} I ds &= \frac{4\beta(p-3)(p+3)}{d\sqrt{d}(p-1)^4}\int_{\xi}\lim_{\xi\to\pm\infty} I ds \\
&= \pm\frac{2^{\frac{-2}{p-1}}\beta(p-3)(p+3)\sqrt{\pi}}{d^2(p-1)^4}\frac{\Gamma\left(\frac{2}{p-1}\right)\Gamma\left(\frac{1}{p-1}\right)}{\Gamma\left(\frac{p+1}{p-1}\right)\Gamma\left(\frac{p+1}{2(p-1)}\right)}e^{\sqrt{d}|\xi|} \\
\frac{4\beta(p-3)}{d\sqrt{d}(p-1)^3}\lim_{\xi\to\pm\infty}\int^{\xi} II ds &= \frac{4\beta(p-3)}{d\sqrt{d}(p-1)^3}\int^{\xi}\lim_{\xi\to\pm\infty} II ds \\
&= \pm\frac{2^{\frac{p-3}{p-1}}\beta(p-3)\sqrt{\pi}}{2d^2(p-1)^3}\frac{\Gamma\left(\frac{1}{p-1}\right)}{\Gamma\left(\frac{p+1}{2(p-1)}\right)}e^{\sqrt{d}|\xi|} \\
\frac{2\beta(p+3)}{d(p-1)^2}\lim_{\xi\to\pm\infty}\int^{\xi} III ds &= \frac{2\beta(p+3)}{d(p-1)^2}\int^{\xi}\lim_{\xi\to\pm\infty} III ds \\
&= \frac{\beta(p+3)}{2d(p-1)^2}\frac{\Gamma\left(\frac{2}{p-1}\right)}{\Gamma\left(\frac{p+1}{2(p-1)}\right)}\xi^2
\end{aligned}
\tag{A.3}
$$

Now we multiply these results with the asymptotic expression (A.2) and obtain that as $\xi \to \pm\infty$

$$
\begin{aligned}
\psi_1\int^{\xi}\psi_2 g ds &= \frac{\beta\sqrt{\pi}(p-3)}{d\sqrt{d}(p-1)^3}\frac{\Gamma\left(\frac{1}{p-1}\right)}{\Gamma\left(\frac{p+1}{2(p-1)}\right)}\left(\frac{d(p+1}{2}\right)^{\frac{1}{p-1}}\left[2-\frac{p+3}{p-1}\frac{\Gamma\left(\frac{2}{p-1}\right)}{\Gamma\left(\frac{p+1}{p-1}\right)}\right] \\
&= -\frac{\beta\sqrt{\pi}(p-3)}{2d\sqrt{d}(p-1)^2}\frac{\Gamma\left(\frac{1}{p-1}\right)}{\Gamma\left(\frac{p+1}{2(p-1)}\right)}\left(\frac{d(p+1}{2}\right)^{\frac{1}{p-1}}
\end{aligned}
$$

Summarising,

$$
\begin{aligned}
& \lim_{\xi\to\pm\infty}\psi_2\left(A_2+\int_0^{\xi}\psi_1 g ds\right)-\psi_1\int^{\xi}\psi_2 g ds \\
& = \frac{1}{2d}\left(\frac{d(p+1)}{2}\right)^{\frac{1}{p-1}}\left[2^{-\frac{2}{p-1}}e^{\sqrt{d}|\xi|}\left(-A_2\left(\frac{d(p+1)}{2}\right)^{-\frac{2}{p-1}}\pm\frac{\sqrt{\pi}\beta(p-5)}{2\sqrt{d}(p-1)^2}\frac{\Gamma\left(\frac{2}{p-1}\right)}{\Gamma\left(\frac{p+3}{2(p-1)}\right)}\right)\right. \\
& \left.\mp\frac{\sqrt{\pi}\beta(p-3)}{\sqrt{d}(p-1)^2}\frac{\Gamma(\frac{1}{p-1})}{\Gamma(\frac{p+1}{2(p-1)})}+\frac{\beta\sqrt{\pi}(p-3)}{\sqrt{d}(p-1)^2}\frac{\Gamma\left(\frac{1}{p-1}\right)}{\Gamma\left(\frac{p+1}{2(p-1)}\right)}\right]+\mathcal{O}(e^{-\sqrt{d}|\xi|})
\end{aligned}
\tag{A.4}
$$

# B Asymptotics of solutions in the intermediate region

In this Appendix we determine asymptotic expressions of the solutions in the intermediate region (4.27) and (4.29) as $|z| \to \infty$. The three integrals for which the asymptotics needs to be determined are given by

$$I_0 = \int_{C_0} t^{\frac{3-p}{p-1}} e^{zt-\frac{1}{12}t^3} dt \tag{B.1}$$

$$I_1 = \int_{\tilde{L}_0} t^{\frac{3-p}{p-1}} e^{zt-\frac{1}{12}t^3} dt \tag{B.2}$$

$$I_2 = \int_{L_1+L_2} t^{\frac{3-p}{p-1}} e^{zt-\frac{1}{12}t^3} dt, \tag{B.3}$$

where the different paths of integration are shown in figure 5.

There are two possible regions of integration that can give a leading order contribution to these integrals. One is the region close to $t = 0$ where the $t^{\frac{3-p}{p-1}}$-factor becomes large since $\frac{3-p}{p-1} < 0$. The other region of attention is that where $t = \mathcal{O}(z^{\frac{1}{2}})$. We determine the asymptotics in the two regions by using different methods. For the region around zero we expand the integrand and for the second region we use the saddle-point method or method of stationary phase.

The paths of integration will be deformed such that the endpoints still remain the same.

We start by determining the asymptotic expressions for large $z$ of integral (B.3). Since $z$ is real, the paths of integration $L_1$ and $L_2$ can be deformed into the imaginary axis. By substituting $t = is$ the integral becomes

$$I_2 = i(-1)^{\frac{3-p}{p-1}} \left[ \int_0^\infty s^{\frac{3-p}{p-1}} e^{i\left(zs+\frac{1}{12}s^3+\frac{(p-3)\pi}{2(p-1)}\right)} ds + \int_0^{-\infty} s^{\frac{3-p}{p-1}} e^{i\left(zs+\frac{1}{12}s^3+\frac{(p-3)\pi}{2(p-1)}\right)} ds \right]. \tag{B.4}$$

By rewriting the second integral and adding the two integrals, we find

$$I_2 = (-1)^{\frac{2}{p-1}} 2 \int_0^\infty s^{\frac{3-p}{p-1}} \sin\left( zs + \frac{1}{12}s^3 + \frac{(p-3)\pi}{2(p-1)} \right) ds. \tag{B.5}$$

We study this integral by splitting in into two parts, one close to zero and one where $t = \mathcal{O}(z^{\frac{1}{2}})$. For this we introduce $z_1$ such that $1 \ll z_1 \ll z^{\frac{1}{2}}$ and write

$$\begin{aligned} I_2 &= \int_0^{z_1} h(s) ds + \int_{z_1}^\infty h(s) ds, \\ &= I_2^{(1)} + I_2^{(2)} \end{aligned} \tag{B.6}$$

where $h(s) = (-1)^{\frac{2}{p-1}} 2 s^{\frac{3-p}{p-1}} \sin\left( zs + \frac{1}{12}s^3 + \frac{(p-3)\pi}{2(p-1)} \right)$.

We are interested in the behaviour of the first integral $I_2^{(1)}$ for $|z| \gg 1$, therefore, we introduce $\varepsilon = \pm\frac{1}{z}$ such that $0 < \varepsilon \ll 1$, where the upper sign corresponds to $z > 0$ and

the minus-sign to $z<0$. After setting $s=\varepsilon y$ in expression (B.5), we obtain

$$\begin{aligned} I_2^{(1)} &= \pm 2(-\varepsilon)^{\frac{2}{p-1}} \int_0^{\varepsilon^{-1}z_1} y^{\frac{3-p}{p-1}} \sin\left(y \pm \frac{\varepsilon^3}{12}y^3 \pm \frac{(p-3)\pi}{2(p-1)}\right) dy \\ &= \pm 2(-\varepsilon)^{\frac{2}{p-1}} \left(\int_0^{\varepsilon^{-1}z_1} y^{\frac{3-p}{p-1}} \sin\left(y \pm \frac{(p-3)\pi}{2(p-1)}\right) dy + \mathcal{O}(|\varepsilon|^3)\right) \\ &= \pm 2(-|z|)^{\frac{2}{p-1}} C(p, \pm D_0)(1+\mathcal{O}(|z|^3)) \end{aligned}$$

where we take an expansion for $\varepsilon \ll 1$. Note that this can be done since in this region of integration$\varepsilon^3 y^3$ is indeed much smaller than $y$.

Now, we study the integral in the above expression separately for some constant $D$

$$\begin{aligned} C(p,D) &= \int_0^{\varepsilon^{-1}z_1} y^{\frac{3-p}{p-1}} \sin(y+D)\, dy \\ &= \int_0^{\varepsilon^{-1}z_1} y^{\frac{3-p}{p-1}} \left[\cos(y)\sin(D) + \sin(y)\cos(D)\right] dy \\ &= \frac{1}{2}\Gamma\left[\frac{2}{p-1}\right] i^{\frac{p-3}{p-1}} \left(-i((-1)^{\frac{p-3}{p-1}}-1)\sin(D) + ((-1)^{\frac{p-3}{p-1}}+1)\cos(D)\right) \\ &= -\frac{1}{2}\Gamma\left[\frac{2}{p-1}\right]\left(e^{i(D-D_0)} + e^{i(D_0-D)}\right) \\ &\quad -\Gamma\left[\frac{2}{p-1}\right]\cos(D-D_0), \end{aligned} \tag{B.7}$$

where $D_0 = \frac{(p-3)\pi}{2(p-1)}$.

Hence, for large $z$,

$$I_2^{(1)} = \mp 2(-|z|)^{-\frac{2}{p-1}}\Gamma\left[\frac{2}{p-1}\right]\cos(\pm D_0 - D_0) + \mathcal{O}(|z|^{-\frac{2}{p-1}-3}), \tag{B.8}$$

where, again, $D_0 = \frac{(p-3)\pi}{2(p-1)}$.

Now, we focus on the second part of the integral, on $I_2^{(2)}$ and apply the method of stationary phase. Again, we take a more general approach and analyse

$$\tilde{I}_2 = \int_{z_1}^{\infty} s^{\frac{3-p}{p-1}} \sin\left(zs + \frac{1}{12}s^3 + D\right) ds.$$

Then, we write the sine-function in complex exponentials and rescale the variables to obtain an integral which is in the form to which the method of stationary phase can be applied. More specifically, for $z>0$, resp $z<0$, we introduce $\lambda^2 = \pm z$ and $s=\lambda r$, then

$$\tilde{I}_2(z) = \frac{1}{2i}\lambda^{\frac{2}{p-1}} \int_{\lambda^{-1}z_1}^{\infty} r^{\frac{3-p}{p-1}} \left(e^{iD}e^{i\lambda^3(\pm r + \frac{1}{12}r^3)} - e^{-iD}e^{-i\lambda^3(\pm r+\frac{1}{12}r^3)}\right) dr. \tag{B.9}$$

where the upper sign corresponds to $z>0$ and the lower sign to $z<0$.

For $z<0$, the method of stationary phase can be directly applied to each of these integrals. The first integral is given by

$$\int_{\lambda^{-1}z_1}^{\infty} r^{\frac{3-p}{p-1}} e^{iD} e^{i\lambda^3(\pm r+\frac{1}{12}r^3)} dr = 2^{\frac{3-p}{p-1}}\sqrt{2\pi}\lambda^{-\frac{3}{2}} e^{i(-\frac{4}{3}\lambda^3+\frac{\pi}{4}+D)}.$$

Then, the contribution of the integrals is added to yield

$$I_2^{(2)(z)} = (-1)^{\frac{2}{p-1}} 2^{\frac{p+3}{2(p-1)}} |z|^{\frac{1}{p-1}-\frac{3}{4}} \sqrt{\pi}\cos\left(\frac{4}{3}|z|^{\frac{3}{2}} + \frac{\pi}{4} - D_0\right),$$

for $z<0$.

For $z>0$, the integrals in (B.9) can be studied with the more general method. Then, it turns out that the leading order contribution of the two integrals cancels, and we conclude that

$$I_2^{(2)} = \mathcal{O}(z^{\frac{1}{p-1}-\frac{9}{4}}).$$

Summarising, we find that

$$I_2 = \begin{cases} -2(-z)^{\frac{-2}{p-1}}\Gamma(\frac{2}{p-1}) + \mathcal{O}(z^{\frac{1}{p-1}-\frac{9}{4}}) & \text{for } z>0 \\ 2(-|z|)^{\frac{-2}{p-1}}\Gamma(\frac{2}{p-1})\cos(\frac{(p-3)\pi}{p-1}) + (-1)^{\frac{2}{p-1}} 2^{\frac{p+3}{2(p-1)}} |z|^{\frac{1}{p-1}-\frac{3}{4}}\sqrt{\pi}\cos\left(\frac{4}{3}|z|^{\frac{3}{2}} + \frac{\pi}{4} - D_0\right) & \text{for } z<0 \end{cases} \tag{B.10}$$

Note that for $p=5$, $\cos(\frac{(p-3)\pi}{p-1}) = 0$, hence the first term for $z<0$ drops out and only the second term remains. On the other hand, when $p>5$, the second term becomes higher order compared to the first one since $\frac{1}{p-1}-\frac{3}{4} < \frac{2}{p-1}$ for $p>5$. Hence, the leading order dynamics is algebraic decaying. This distinction between the behaviour of the solutions between $p=5$ and $p>5$ will lead to a different matching analysis and also to different behaviour of the final solutions.

When studying the integral $I_0$ we use that $C_0$ can be transformed to correspond to the imaginary axis and then the integral is given by

$$I_0 = 2i(-1)^{\frac{3-p}{p-1}} \int_0^{\infty} s^{\frac{3-p}{p-1}} \sin\left(zs + \frac{1}{12}s^3 + \frac{(p-3)\pi}{2(p-1)} + \frac{\pi}{2}\right) ds. \tag{B.11}$$

In a similar way as before in (B.6) we split this integral into two parts, $I_0^{(1)}$ and $I_0^{(2)}$.

To determine the integral $I_0^{(1)}$ around zero, we can apply expression (B.7). Also, we use that $C(p, D_0+\frac{\pi}{2}) = 0$ for all $p$ so that $I_0^{(1)}$ gives no leading order contribution for $z>0$.

When studying the integral $I_0^{(2)}$, we in a similar way as before, rescale integration variables and apply the saddle point method.

Summarising, we find that

$$I_0 = i(-1)^{\frac{3-p}{p-1}} 2^{\frac{5-p}{2(p-1)}} z^{\frac{1}{p-1}-\frac{3}{4}} e^{-\frac{4}{3}z^{\frac{3}{2}}} \left(1 + \mathcal{O}\left(z^{-\frac{3}{2}}\right)\right) \text{ for } z>0 \tag{B.12}$$

$$I_0 = (-1)^{\frac{3-p}{p-1}} i \left(2|z|^{\frac{-2}{p-1}}\Gamma\left(\frac{2}{p-1}\right)\cos(-2D_0 - \frac{\pi}{2}) + 2^{\frac{p+3}{2(p-1)}}|z|^{\frac{1}{p-1}-\frac{3}{4}}\sqrt{\pi}\cos\left(\frac{4}{3}|z|^{\frac{3}{2}} - \frac{\pi}{4} - D_0\right)\right) \text{ for } z<0$$

where as before $D_0 = \frac{(p-3)\pi}{2(p-1)}$. Note that there is again a distinction between the behaviour of the solution for $p = 5$ and $p > 5$ when $z < 0$ as was the case for $I_2$. Now, the terms are for $p = 5$ of the same order, whereas the second term becomes higher order compared to the first term for $p > 5$.

The integral $I_1$ is given by

$$I_1 = \int_0^\infty t^{\frac{3-p}{p-1}} e^{zt - \frac{1}{12}t^3} dt.$$

For $z > 0$, in the region for large $t$ the integral is found by using Laplace's method, yielding an exponentially growing term. The integral around zero is determined by using the fact that the cubic term in the exponential is higher order compared to the linear term. Hence,

$$\begin{aligned} I_1^{(1)} &= \int_0^{z_2} t^{\frac{3-p}{p-1}} e^{zt} dt \\ &= \left[\frac{p-1}{2} t^{\frac{p-1}{2}} e^{zt}\right]_0^{z_2} - \int_0^{z_2} \frac{p-1}{2} t^{\frac{p-1}{2}} z e^{zt} dt \\ &= \frac{p-1}{2} z_2^{\frac{p-1}{2}} e^{zz_2}, \end{aligned}$$

to leading order, where we restrict to $z_2 \ll z^{-1}$. Thus, $I_1^{(1)} \ll I_1^{(2)}$.

When $z < 0$, the main contribution to the integral comes from the region around zero. By using Watson's Lemma we find that

$$I_1 = I_1^{(1)} + hot = \int_0^{z_1} t^{\frac{3-p}{p-1}} e^{-|z|t} dt = \Gamma(\frac{2}{p-1}) |z|^{-\frac{2}{p-1}},$$

to leading order.

Concluding we find,

$$\begin{aligned} I_1 &= 2^{\frac{5-p}{2(p-1)}} z^{\frac{1}{p-1} - \frac{3}{4}} e^{\frac{4}{3}z^{\frac{3}{2}}} \left(1 + \mathcal{O}\left(z^{-\frac{3}{2}}\right)\right) \quad \text{for } z > 0 \\ I_1 &= \Gamma(\tfrac{2}{p-1}) |z|^{-\frac{2}{p-1}} \qquad\qquad\qquad\qquad\quad \text{for } z < 0. \end{aligned} \tag{B.13}$$

# References


[1] M.J. Ablowitz, M. Kruskal, and H. Segur. A note on Miura's transformation. *J. Math. Phys.*, 20:999 – 1003, 1979.

[2] M. Abramowitz and I. A. Stegun. *Handbook of Mathematical Functions with Formulas, Graphs, and Mathematical Tables.* Dover, New York, 1964.

[3] T.B. Benjamin. Lectures on nonlinear wave motion. *Lectures in applied math*, 15:AMS, 1974.

[4] T.B. Benjamin, J.L. Bona, and J.J. Mahoney. Model equations for long wave nonlinear dispersive media. *Philos. Trans. Roy. Soc. London Ser. A*, 272:47 – 78, 1971.

[5] J.B. van den Berg, J. Hulshof, and J.R. King. Formal asymptotics of bubbling in the harmonic map heat flow. *SIAM J. Appl. Math.*, 63:1682 – 1717, 2003.

[6] J. L. Bona, P. E. Souganidis, and W. A. Strauss. Stability and instability of solitary waves of Korteweg-de Vries type. *Proceedings of the Royal Society of London. A. Mathematical and Physical Sciences*, 411(1841):395 – 412, 1987.

[7] J.L. Bona, V.A. Dougalis, O.A. Karakashian, and W.R. McKinney. Conservative high-order numerical schemes for the generalized Korteweg-de Vries equation. *Philos. Trans. Roy. Soc. London Ser. A*, 351:107 – 164, 1995.

[8] D. B. Dix and W. R. McKinney. Computations of self-similar blow-up solutions of the generalized Korteweg-de Vries equation. *Differential and Integral Equations*, 11:679 – 723, 1998.

[9] D.J. Korteweg and G. de Vries. On the change of form of long waves advancing in a rectangular canal, and on a new type of long stationary waves. *Philosophical Magazine*, 5(39):422 – 443, 1895.

[10] P. D. Lax. Integrals of nonlinear equations of evolution and solitary waves. *Communications on pure and applied mathematics*, 21:467–490, 1968.

[11] Y. Martel and F. Merle. Instability of solitons for the critical generalized Korteweg-de Vries equation. *Geom. Funct. Anal.*, 11:74 – 123, 2001.

[12] Y. Martel and F. Merle. Blow up in finite time and dynamics of blow up solutions for the $l^2$-critical generalized KdV equation. *J.Amer. Math. Soc.*, 15:617–664, 2002.

[13] Y. Martel and F. Merle. Stability of blow-up profile and lower bounds for blow-up rate for the critical generalized KdV equation. *The Annals of Mathematics*, 155(1):235–280, 2002.

[14] F. Merle. Existence of blow-up solutions in the energy space for the critical generalized KdV equation. *J.Amer. Math. Soc.*, 14:555 – 578, 2001.

[15] R.M. Miura. The Korteweg-de Vries equation: A survey of results. *SIAM Review*, 18(3):412 – 459, 1976.

[16] R.L. Pego and M.I. Weinstein. Asymptotic stability of of solitary waves. *Comm. Math. Phys.*, 164:305 – 349, 1994.

[17] W.H. Reid. Integral representations for products of Airy functions. *Zeitschrift für Angewandte Mathematik und Physik*, 48 (4):646 – 655, 1995.

[18] V. Rottschäfer. Asymptotic analysis of a new type of multi-bump, self-similar, blowup solutions of the Ginzburg-Landau equation. *European Journal of Applied Mathematics*, 24:103 – 129, 2013.

[19] P. Saucez, A. Vande Wouwer, and P.A. Zegeling. Adaptive method of lines solutions for the extended fifth order korteweg-de vries equation. *J. of Comp. & Appl. Maths.*, 183:343 – 357, 2005.

[20] O. Vallée. On the linear third order differential equation. *Lecture Notes in Physics, Dynamical systems, Plasmas and Gravitation*, 518:340 – 347, 1999.

[21] F. Merle Y. Martel. A Liouville theorem for the critical generalized Korteweg-de Vries equation. *J. Math. Pure Appl.*, 79:339 – 425, 2000.

[22] N.J. Zabusky. Fermi-Pasta-Ulam, solitons and the fabric of nonlinear and computational science: History, synergetics, and visiometrics. *Chaos*, 15:015102, 2005.